IEEE Access
Multidisciplinary ⋮ Rapid Review ⋮ Open Access Journal

Received 27 August 2024, accepted 11 September 2024, date of publication 13 September 2024,
date of current version 26 September 2024.

Digital Object Identifier 10.1109/ACCESS.2024.3460671

RESEARCH ARTICLE

Experimental Investigation of All-Optical Sub-THz Wavelength Conversion for 6G Communication Systems

YAZAN ALKHLEFAT[1], MAGED A. ESMAIL[2], AMR M. RAGHEB[3], SEVIA MAHDALIZA IDRUS[1], (Senior Member, IEEE), FARABI M. IQBAL[1], AND SALEH A. ALSHEBEILI[3]

[1]Department of Electrical Engineering, Universiti Teknologi Malaysia, Johor Bahru 81310, Malaysia
[2]Department of Communications and Networks Engineering and Smart Systems Engineering Laboratory, Prince Sultan University, Riyadh 12435, Saudi Arabia
[3]Department of Electrical Engineering, King Saud University, Riyadh 11421, Saudi Arabia

Corresponding author: Yazan Alkhlefat (amyazan1988@graduate.utm.my)

This work was supported by the Researchers Supporting Project, King Saud University, Riyadh, Saudi Arabia, under Grant RSP2024R46.

ABSTRACT Sub-terahertz (sub-THz) waves, operating in the 0.1-1 THz band, offer significant potential for next-generation 6G systems. These systems stand to benefit from photonic technologies that enable terabits-per-second communication with low latency and high throughput. This paper introduced, for the first time, a semiconductor optical amplifier (SOA) as a fast and reliable photonic-based technique for sub-THz wavelength conversion in fiber-based networks. The wavelength conversion leveraged nonlinear phenomena in the SOA, including cross-gain modulation, self-phase modulation, and four-wave mixing effects. Numerical simulations demonstrated an all-optical wavelength conversion capable of handling 100-GHz sub-THz signals with 16-ary quadrature amplitude modulation formats, achieving a data rate switching of 5 Gbps. Key system parameters were optimized, resulting in a 28.7 dB suppression ratio for the generated optical single sideband (OSSB) signal. Additionally, a proof-of-concept laboratory experiment validated the THz signal-switching concept. The proposed system incorporated a hybrid fiber/wireless channel and utilized various measures for performance evaluation.

INDEX TERMS 6G, optical single sideband (OSSB), photonic switching, sideband suppression ratio (SSR), semiconductor optical amplifier (SOA), terahertz communication (THz).

I. INTRODUCTION

The increasing need for high-speed wireless networks and large-bandwidth applications like cloud computing, the Internet of Things (IoTs), and ultra-high definition (UHD) video streaming have motivated the employment of sub-terahertz (THz) frequency bands for future next-generation 6G communication systems [1]. For instance, video traffic has increased by 66% between 2018 and 2023 [2]. Also, mobile data traffic increased eightfold within the same period [3]. Currently, the traffic for mobile and wireless devices occupies 71% of the total traffic [4]. Moreover, the data rates usage of wireless systems will be enough to compete with wired broadband by 2030 [5]. The prediction of the wireless network capacity will exceed 100 Gbps during the next 7 years [6]. Following this trend, the data rate of wireless systems will reach terabits per second (Tbps) in the coming decade. However, current spectral resources allocated in the microwave (MW) or millimeter-wave (MMW) bands are no longer enough for the data capacity of Tbps that is expected to be provided in the next ten years. So ultra-broadband wireless systems within the THz band are being actively investigated worldwide toward the future 6G era. This THz band lies in the range between 100 GHz (3 mm) and 10 THz (30 μm) [7], [8], [9], [10], [11], [12], [13], [14], [15], [16].

Using the THz band for wireless communication poses challenges. One significant hurdle is the high propagation

The associate editor coordinating the review of this manuscript and approving it for publication was Miguel López-Benítez.

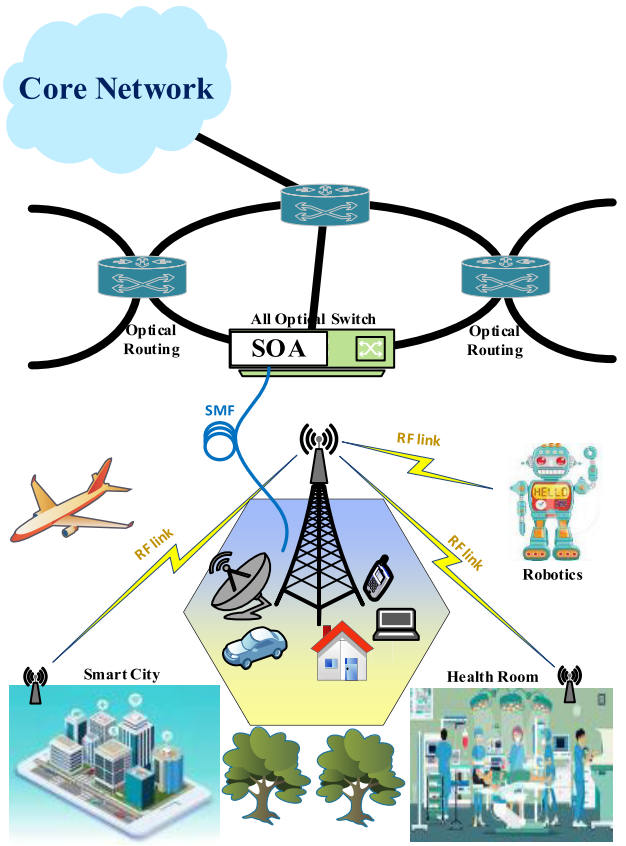

FIGURE 1. A conceptual figure for a 6G network includes a photonics-based switching for THz signals.

loss caused by atmospheric attenuation, which leads to a limited communication range. Overcoming this challenge is paramount to unlocking THz wireless communication's full potential. One practical solution is to transmit the THz signal over optical links in the backhaul. Using optical wavelengths will require wavelength conversion for efficient signal routing in the optical network. Fig. 1 displays the concept of THz switching in a 6G network. Various types of devices are connected to the 6G base station using THz bands. In the backhaul, the base station transmits the traffic over optical fiber to the metro network, where an optical switch is mandatory to perform wavelength conversion and switching to avoid wavelength mixing in the optical network.

In general, two technologies can implement the wavelength conversion of optical signals [17], [18]: photonics-based and electronics-based techniques. From a device perspective, it can be categorized as follows: semiconductor optical amplifier (SOA) and lasers (LD), electro-absorption modulator (EAM), electro-optic crystal, and optical fiber. Generally, SOA and EAM offer the advantages of small size (∼1 mm) and low operational power, while the electro-optic crystal has a larger size (∼50 mm) and the optical fiber can reach distances of hundreds of kilometers [19]. Wavelength conversion using SOA is the most popular method as it can support very high-speed conversion with nanosecond-level rise or fall time and provides optical gain performance. Additionally, SOA can be integrated with other optical components and offers polarization independence and a large extinction ratio [19], [20].

Over the past two decades, there has been considerable research interest in all-optical wavelength conversion and switching (AOWC) using SOA techniques, driven by its distinct advantages in enhancing network flexibility and supporting long transmission distances [17]. Several advantages have been gained by exploiting photonics-based wavelength conversion using SOA over electronic devices. These include (i) high instantaneous bandwidth, (ii) modulation format transparency, and (iii) low latency. Moreover, an advantage can be achieved by using photonics-based techniques, ensuring a higher modulation order gained due to the conversion of optical to THz with high-speed amplitude and photo mixing. Furthermore, photonic devices can easily assign multi-carrier transmission by adding an optical fiber laser to the main optical signals. As mentioned before, the THz communication system can provide high data rates wirelessly using photonics-based techniques [19].

Over the past two decades, there has been notable research attention towards all-optical signal processing for wavelength conversion [17], [21], [22], [23], [24], [25], [26], [27]. The wavelength conversion, switching, and routing of THz signal in the communication networks is a realistic example where the SOA is considered a helpful wavelength converter by exploiting its non-linear effects, such as four-wave mixing (FWM), self-phase modulation (SPM), and cross-gain modulation (XGM) [28]. In this context, we can define wavelength converters as optical devices that transfer data signals from one wavelength to the desired wavelength in the network according to the application used. Therefore, SOA can be considered the primary device for this function, enabling all-optical switching and wavelength conversion. For example, it can convert the optical signal wavelength in the optical domain from the current wavelength to the new required wavelength with no requirement to convert it to the electrical domain and then back into the optical domain [29], [30]. Moreover, eliminating the electronic components in the conversion process enhances the system by reducing the consumed power and cost and removing the bandwidth limitation in the electronic devices [28].

In the literature, researchers often use the SOA as a wavelength converter for a single carrier. For example, the authors in [31] presented SOA-based wavelength switching for a 50-GHz millimeter wave (MMW) signal carries two 5G modulation schemes: filtered bank multi-carrier-offset quadrature amplitude modulation (FBMC-OQAM) and universal filtered multi-carrier (UFMC). The system's parameters were optimized to obtain an optical single sideband signal (OSSB) with a sideband suppression ratio (SSR) of 18.85 dB. Reference [17] discussed an examination of an all-optical burst mode wavelength converter employing the SOA-Mach-Zehnder Interferometer (SOA-MZI).

Besides, in [29], a 30-GHz MMW switching system using SOA was proposed, where a data rate of 3-Gbaud and quadrature phase shift keying (QPSK) signal was switched. In that work, the radio over fiber (RoF) system is not considered and the obtained SSR was 14 dB.

In [32], the authors presented the optical switching of K-band 5G signal experimentally using cascaded SOAs considering RoF with two different SMF lengths (12 and 31 km) where the achieved power penalty was ∼0.5 dB. In [20], a 20 GHz microwave carrier carrying a 16-QAM signal was switched using SOA while implementing RoF system with 9 km SMF, where the achieved SSR of the converted signal was 22.65 dB for down-conversion and 17.85 dB for up-conversion. Also, the authors in [33] optimized the system's parameters in a wavelength conversion system in terms of SOA's optical power and injection current. The demonstration did not include RoF system; it showed the conversion of an E-band signal operating at 80 GHz and carrying 7 Gbps. In [34], the authors reported a 128-QAM modulation format for wavelength conversion using SOA with a 227 Gbps data rate by simulation utilizing Optisystem numerical simulation software. The authors analyzed the performance in terms of optical signal-to-noise ratio, bandwidth, and injection current parameters.

In [35], the authors used numerical software to investigate the wavelength spacing between pump wavelength and probe wavelength in a wavelength conversion system with a 9 Gbps QPSK signal centered at 30 GHz carrier frequency without RoF demonstration. The results showed that the optimum spacing value is equal to 1.6 nm. In [36], an OSSB switching with an up-conversion scheme in SOA is experimentally demonstrated to transmit a data rate of 10 Gb/s at 60 GHz carrier frequency of 16 QAM orthogonal frequency division multiplexing (OFDM) signal with RoF system using 20 km SMF. The authors in [37] utilized simulation software to examine the performance of a 5G modulation format called the generalized frequency division multiplexing (GFDM) without RoF consideration. They specifically focused on generating an OSSB signal using SOA with a carrier frequency of 40 GHz. The optical double-sideband (ODSB) and OSSB signals were investigated in that work.

Table 1 summarizes the literature review of wavelength switching considering key parameters, including the carrier frequency, modulation format, SSR, and data rate. It is clear from the previous discussion that the THz signal switching has not yet been investigated. Therefore, in this work, we fill in that gap and propose a RoF wavelength conversion model for THz signals using SOA. We utilize the SOA's nonlinear phenomena to produce and convert an efficient OSSB signal to the required wavelength. Toward that objective, the key parameters that control the efficiency of wavelength switching are thoroughly investigated. This includes the SOA's injection current, the power of the pump and probe lasers, and SSR. In addition, a lab's proof-of-concept experiment is also conducted.

TABLE 1. Comparison between implemented wavelength conversion systems.

Ref.	Modulation Format	Data Rate (Gbps)	Carrier freq. (GHz)	SSR (dB)
[20]	16-QAM	0.1	20	22.6
[28]	FBMC-16-OQAM	3	30	18.4
[29]	QPSK	6	30	14
[32]	QPSK/16-QAM	6	25	*
[33]	OFDM	7	80	22.91
[35]	QPSK	9	30	*
[36]	OFDM-16QAM	10	60	**
[37]	GFDM	5	40	24.33
[38]	OFDM-16QAM	10	30	22.2
This work	16-QAM/QPSK	5/4	100	28.7

* SSR was not measured.
** The specific value is not provided in the paper.

The remainder of the paper is organized as follows: The system setup and numerical simulation results are discussed in section II. A proof-of-concept of THz wave wavelength conversion using SOA experiment is presented in section III. Finally, the paper concludes in section IV.

II. SIMULATION RESULTS AND DISCUSSION

In this section we investigate the performance of the SOA in switching THz signals using numerical simulation. The simulation will assist in identifying the key parameters that play a dominant role in the proof-of-concept experimental setup. The mathematical system modeling can be found somewhere else [28], [29], [31].

The nonlinear effects of SOA result from changes in carrier density induced by input signals. These non-linear effects are used in wavelength conversion in high-speed photonic networks. The main forms of nonlinearity in SOA are FWM, XGM, and SPM.

The FWM phenomenon arises from the nonlinear interaction between two input signals injected into the SOA, resulting in the generation of two additional new signals with different frequency components as shown in the output of the SOA in Fig. 2. Three mechanisms contribute to the generation of FWM signals: (i) spectral hole burning (SHB), (ii) carrier heating (CH), and (iii) carrier density modulation (CDM) [39]. FWM can be utilized in various applications such as AOWC [40] and dispersion compensator. Moreover, FWM enables phase conjugation and supports multi-channel operation [41]. On the other side, FWM suffers from some issues like low conversion efficiency, amplified spontaneous emission (ASE) noise from SOA, and polarization sensitivity [42]. When two optical signals are injected to an SOA, the carrier density variations in the active region of SOA affect both signals due to broad spectrum of material gain. The technique which allows the optical signal conversion is XGM. In XGM devices, a strong control signal (probe) modulates the carrier density of the SOA, thereby also modulating a second signal (pump). Therefore, the control modulation on the second signal can be imposed by XGM effect. This method, which inverts the control pulse shape can be applied in wavelength conversion application, affirming that SOA

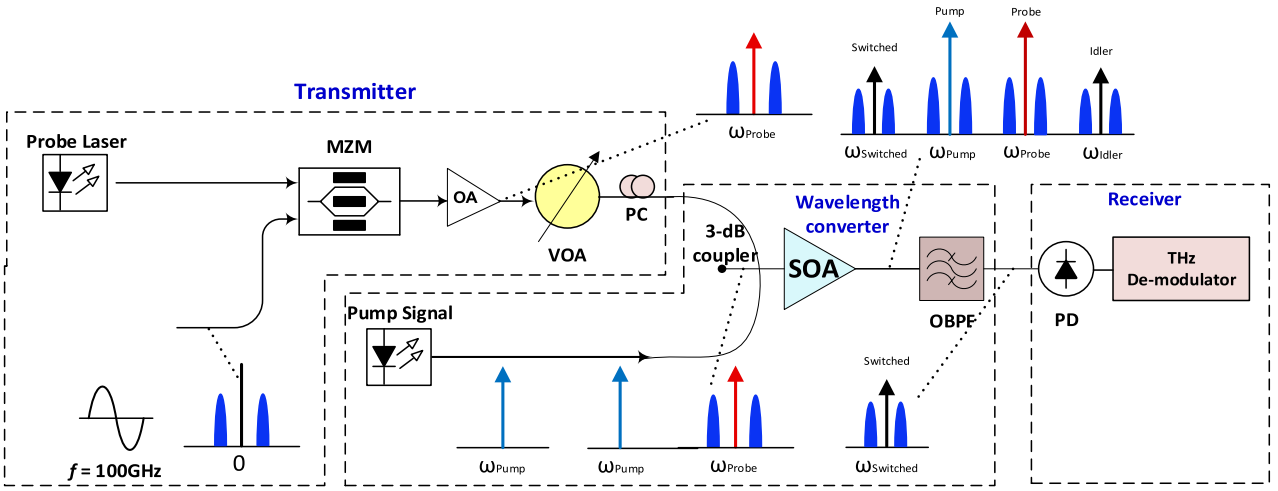

FIGURE 2. Simulation setup of the photonic THz signal wavelength conversion and obtaining OSSB. MZM: Mach Zehnder Modulator. OA: Optical Amplifier. VOA: Variable Optical Attenuator. PC: Polarization Controller. SOA: Semiconductor Optical Amplifier. OBPF: Optical Band Pass Filter. PD: photodetector.

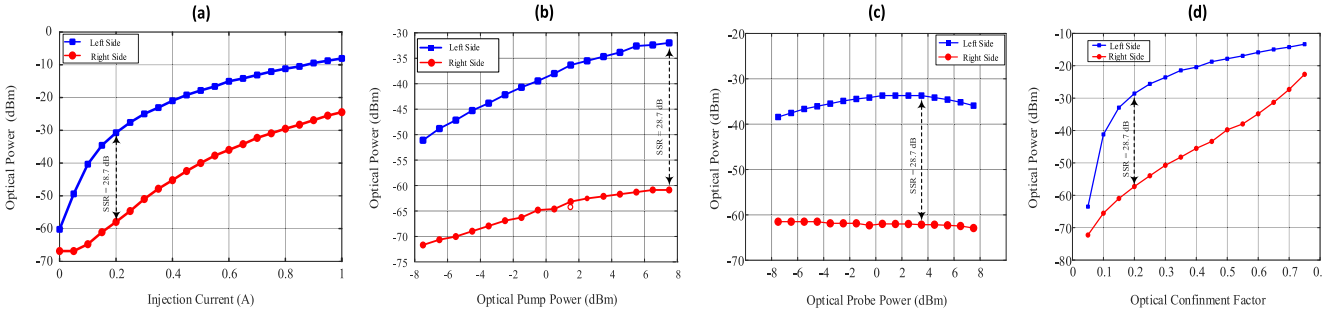

FIGURE 3. Optimization results for the main system parameters: (a) Injection current, (b) Optical pump power, (c) Optical probe power, and (d) Optical confinement factor.

can be used as a wavelength converter [43], [44], [45]. It is important to note in this context that the information from the input signal (probe) is transferred to the converted optical signal (switched). SPM is a key nonlinear phenomenon causing optical pulse spectral broadening. This effect was initially investigated in SOAs as early as 1989. Researchers identified that gain saturation within SOAs is the underlying physical mechanism driving SPM, resulting in refractive index changes dependent on signal intensity and carrier density fluctuations [46].

Figure 2 shows the simulation setup, which is implemented using *VPITransmissionMaker* Ver. 11.1. It has three core parts: the transmitter, the wavelength converter (WC), and the receiver. Firstly, the transmitter generates a 5- Gbps 16-QAM electrical sub-THz signal operating at 100 GHz radio frequency. A continuous laser (CW) is modulated by this signal using MZM, called probe laser, operating at a wavelength of 1552.52 nm with a power of 3.5 dBm and a linewidth <1 kHz. The MZM has an extinction ratio (ER) of 35 dB. The MZM output signal called the probe signal, is then amplified using an optical amplifier and then launched to the second stage, which is the WC. The WC includes the SOA and a CW laser source, called pump signal, operating at 1550.12 nm wavelength and has 7.5 dBm output power. The probe signal is coupled using a (50:50) optical coupler with the pump signal. These two optical beams (i.e., the pump and probe) are then injected into the SOA. At this stage, the SOA's nonlinear effects are exploited to perform the wavelength conversion, where the sub-THz signal is converted to a new wavelength (i.e., switched signal). A polarization controller (PC) and a variable power controller (VOA) are used to control the probe signal's polarization and power, respectively. The output of the SOA will include four signals due to FWM phenomena as indicated in the inset in Fig. 2. The tunable optical filter (TOF) is adjusted to select the switched signal, which carries the THz signal at a frequency of 1547.72nm. The switched signal has a different wavelength than the probe signal. Then, in the last stage, a photodiode (PD) is used to obtain the sub-THz signal. This signal is then analyzed to measure the performance of the switching operation. Table 2 summarizes the simulation setup parameters and their values.

In order to avoid chromatic dispersion in the system, the SOA can be controlled to suppress one of the sidebands that were generated by the MZM. The SSR metric is used to measure the suppression ratio, which can be defined as

TABLE 2. Simulation parameters' values.

Modulation Format	Value
Modulation Order	16-QAM
RF Carrier Frequency	100 GHz
RF Power	-3 dBm
Signal Data Rate	5 Gbps
Probe Signal wavelength	1552.52 nm
Probe Signal Power	variable
Pump Signal wavelength	1550.12 nm
Pump Signal Power	variable
Extinction Ratio for MZM	35 dB
Responsivity of PD	0.15 A/W
SOA's Parameters	
Injection Current (IC)	variable
Height	80 µm
Length	500 µm
Width	3 µm
Optical confinement factor	variable
Index to Gain Coupler	5
Waveguide loss coefficient	4000 1/m

TABLE 3. Optimized system parameters.

Main Parameter	Value
Injection Current	200 mA
Pump Signal Power	7.5 dBm
Probe Signal Power	3.5 dBm
Optical confinement factor	0.2

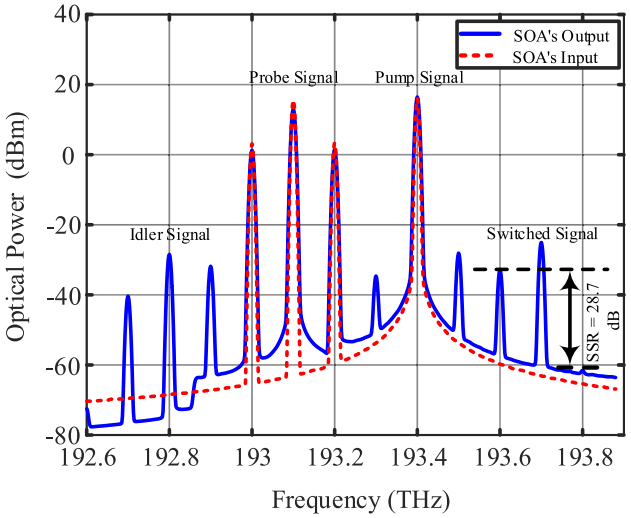

FIGURE 4. The spectrum of the input and output signals of the SOA for wavelength conversion of 100 GHz THz carrier.

the difference in power between the two sidebands (left and right) around the carrier. A high SSR value means better suppression of the sideband. To obtain a high-performance OSSB THz signal with a high SSR value, we need to optimize the main system's parameters, which are listed in Table 3.

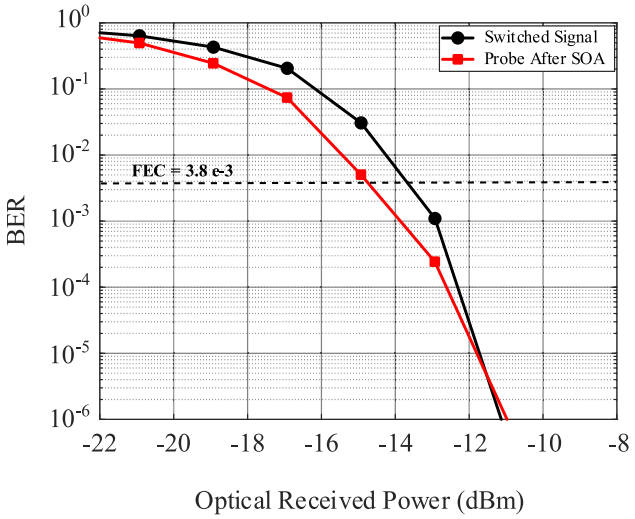

FIGURE 5. BER results versus the received optical power for the probe signal after SOA and switched signal.

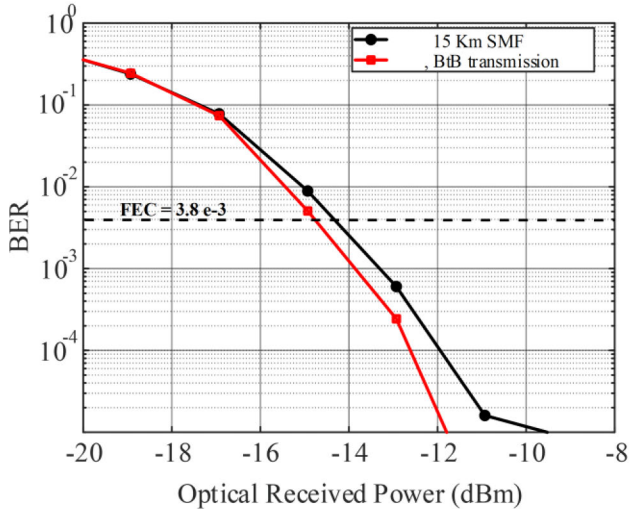

FIGURE 6. Performance of the 16-QAM THz converted signal in terms of BER vs. the optical received power in BtB transmission and 15 km SMF transmission.

In addition, the optimization process will target achieving a switched signal with high power. The process includes optimizing them one by one. In the following, we explain the impact of each parameter on the switched signal.

Figure 3 shows the optical power of the two sidebands versus the four parameters under study. We select the parameter's value that achieves a high SSR. Fig. 3 (a) illustrates the effect of SOA's injection current on SSR. We can see that the maximum SSR is achieved at 200 mA, which corresponds to 28.7 dB SSR. In Fig. 3 (b), the pump signal effect is investigated. The optimum value for its power is 7.5 dBm, which corresponds to 28.7 dB SSR. Similarly, we investigated the effect of the probe power on the SSR metric. The pump power is fixed at 7.5 dBm. Fig. 3 (c) shows the SSR of the switched signal as a function of the

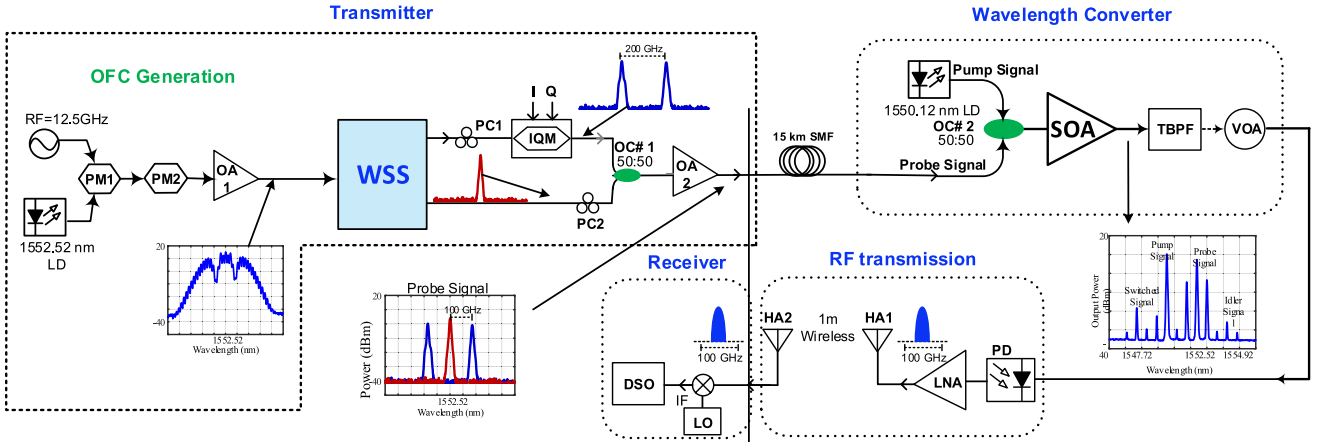

FIGURE 7. Experimental setup for the proposed photonic-based THz wavelength conversion system using SOA. PM: Phase Modulator. OC: Optical Coupler. OA: Optical Amplifier. SOA: Semiconductor Optical Amplifier. WSS: Wavelength Selective Switch. PC: Polarization Controller. TBPF: Tunable Band Pass Filter. PD: photodetector. LNA: Low Noise Amplifier. DSO: Digital Storage Oscilloscope. WC: Wavelength Conversion. OFC: Optical Frequency Comb.

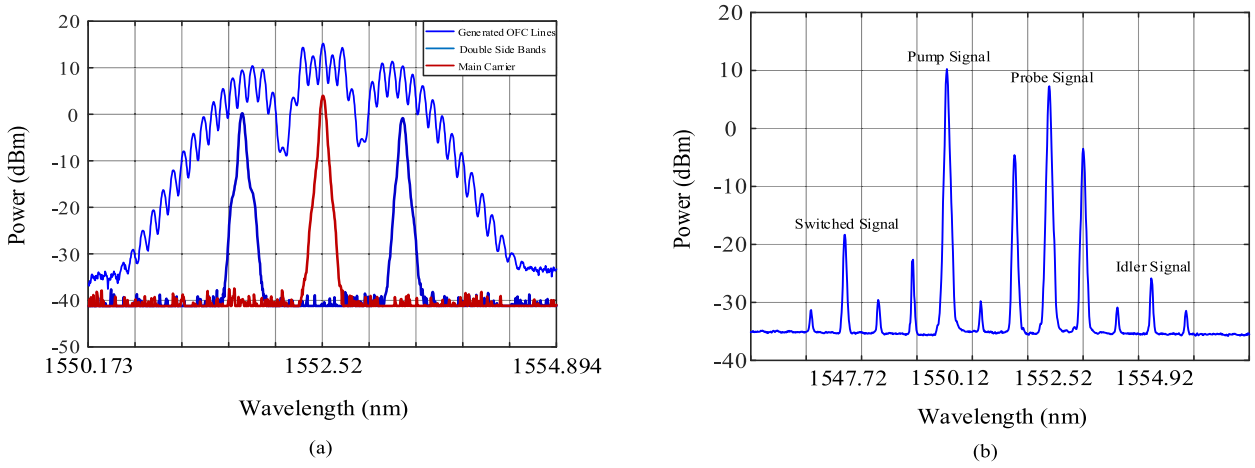

FIGURE 8. (a) WSS input and output signals, and (b) Optical spectrum of SOA's output for down-conversion.

probe power. The maximum achieved SSR is 28.7 dB at 3.5 dBm optical probe power. Finally, the optical confinement factor (Γ) of the SOA is examined with respect to SSR in Fig. 3(d). As can be seen, the optimum value of Γ, which gives maximum SSR, is 0.2.

Table 3 summarizes the corresponding optimum values of the SOA's main parameters.

Next, we exploited the optimized parameters' values in Table 3 to investigate the optical spectrum of the SOA output signal using an optical spectrum analyzer (OSA). This OSA has 0.05 nm bandwidth resolution. The spectrum of the input signal to the SOA (red curve) and the output signal (blue curve) is illustrated in Fig. 4. The input signal spectrum includes the pump signal and the probe signal with the THz signal represented by two sidebands around the probe signal wavelength.

The SOA's output signal in Fig. 4 shows four output signals with their THz sidebands that resulted from the nonlinear effects in the SOA. The THz signal is switched from the probe signal at 1550.52nm wavelength to the switch signal at 1547.72nm wavelength. The separation between all four generated signals is uniform and equals 300 GHz.

The SSR of the output switched signal is high, 28.7 dB, reflecting the excellent sideband suppression to generate an OSSB. In addition, we notice from Fig. 4 that the carried information data by the probe signal is reproduced successfully at two newly generated signals (switched signal and idler signal). Furthermore, the modulation is transferred to the switched signal due to the XGM effect of the SOA.

The performance of the switched signal has been evaluated at the receiver. Fig. 5 shows the BER results versus the total input power to the PD for the probe and switched signals, where both carry the modulated THz signal. At the hard-decision forward error correction (HD-FEC) limit, i.e., BER $= 3.8 \times 10^{-3}$ [47], the switched signal suffers of ∼1 dB power penalty compared to the probe signal. This shows that the THz switched signal is affected minimally by the

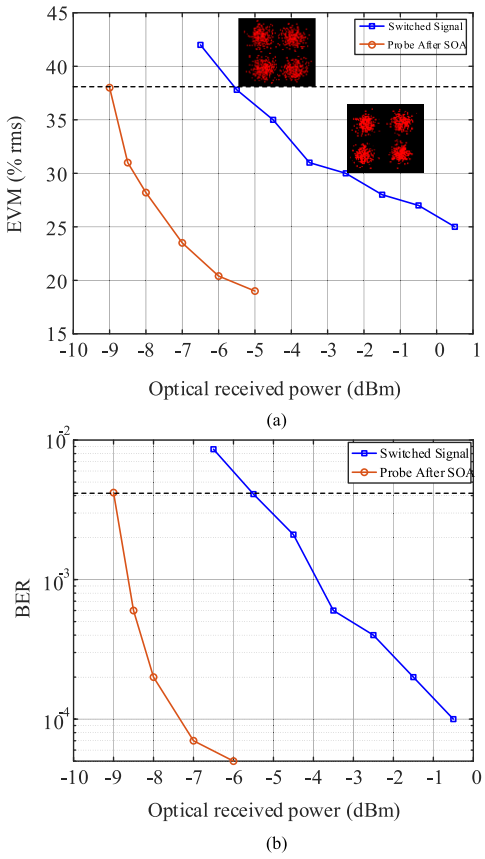

FIGURE 9. (a) EVM and (b) BER versus the received optical power for QPSK Switched THz signal and probe after SOA over BtB transmission for down-conversion. The hybrid transmission link is 15 km SMF and 1 m wireless channel.

switching operation, resulting in a negligible impact on its quality.

The performance of 16-QAM THz switched signal is studied in two scenarios: back-to-back (BtB) transmission and 15 km SMF transmission. This is achieved by measuring BER versus the optical received power at the PD, as shown in Fig. 6. As indicated in the figure, there is a minimal power penalty of ∼0.5 dB at the FEC limit for 15 km SMF transmission compared with BtB transmission. Also, we can see that the BER decreases with the increase of optical power.

The previous discussion shows that the switched signal, i.e., the 5 Gbps 16 QAM signal, is affected by nonlinearities in the switching process. Therefore, the data rate is limited by the conversion process. It is noteworthy that similar bandwidth constraints have been documented in the literature for mmW band applications, as outlined in Table 1. However, it is important to emphasize that achieving higher bandwidth is feasible without the need for wavelength conversion.

III. MATH PROOF-OF-CONCEPT EXPERIMENTAL SETUP AND RESULTS

A proof-of-concept experimental setup for the proposed photonic-based sub-THz wavelength conversion system using SOA is shown in Fig. 7. It includes four sections: transmitter, wavelength converter, RF wireless channel, and receiver. In the transmitter, an optical frequency comb (OFC) is used to generate optical carriers. The main component is the CW laser diode (Koheras ADJUSTIK), which is a low-noise single-frequency laser operating at 1552.52 nm wavelength with 16 dBm an output power and line width < 1 kHz. It is connected to two cascaded phase modulators (PMs) (Eospace), which are driven by a 12.5 GHz RF signal that is generated from an analog signal generator (Keysight E8267D) with an RF power of 11.3 dBm. The PMs generate a comb of optical carriers separated by 12.5 GHz.

Then, the generated OFC carriers are amplified using an optical amplifier (OA1) and launched into a wavelength selective switch (WSS) (FINISAR waveshaper 4000s). The WSS selects three main carriers with a separation of 100 GHz. One carrier is baseband with no modulation, and the two other carriers, which are separated by 200 GHz, are modulated with an IQ modulator (FUJITSU 78110). The modulator modulates these two optical subcarriers with a 4 Gbps QPSK signal.

Then, the modulated and unmodulated carriers are combined using an optical coupler (OC1) and amplified using an OA2 (Amonics AEDFA-PA-40-B-FA). Polarization controllers (PCs) are used to control optical signal polarization.

The output of the transmitter is an optical signal modulated by a 100 GHz signal as indicated in the insets of Fig. 7. The spectrum of the input signal to the WSS and the modulated optical output signal of the transmitter is shown in Fig. 8(a).

The double sideband output signal of the transmitter represents the probe signal at 1552.52 nm. The probe signal is transmitted over a 15 km SMF and then combined using a 50:50 optical coupler (OC2) with a pump signal, generated using a laser diode source (Agilent N7714A) at the 1550.12 nm wavelength. Thereafter, the combined signal is launched into the SOA (Kamelian SOA-NL-L1-C-FA 10-08-022019) to start the WC process, as down-conversion. The SOA's output is shown in Fig. 8(b) using the optical spectrum analyzer OSA (Agilent 86142B), which has a 0.06 nm resolution bandwidth. It is seen that the wavelength conversion for the sub-THz signal at 100 GHz is successfully implemented, where the new switched signal is converted into a wavelength of 1547.72 nm with the same data information as the probe signal. After the wavelength conversion is achieved, the switched signal is filtered using an optical narrow band tunable bandpass filter (TBPF) (EXFP-XTM-50). A variable optical controller (VOA) is used to control the power of the input signal to the PD.

The output of the wavelength converter is launched into a high-speed 100 GHz PD (Finisar BPDV412xR) with responsivity> 0.35 A/W to obtain the 100 GHz electrical sub-THz switched signal. Then, the sub-THz signal is amplified using QuinStar amplifier (QLW-24403336-J0), which is a low noise amplifier. The output of the amplifier is transmitted

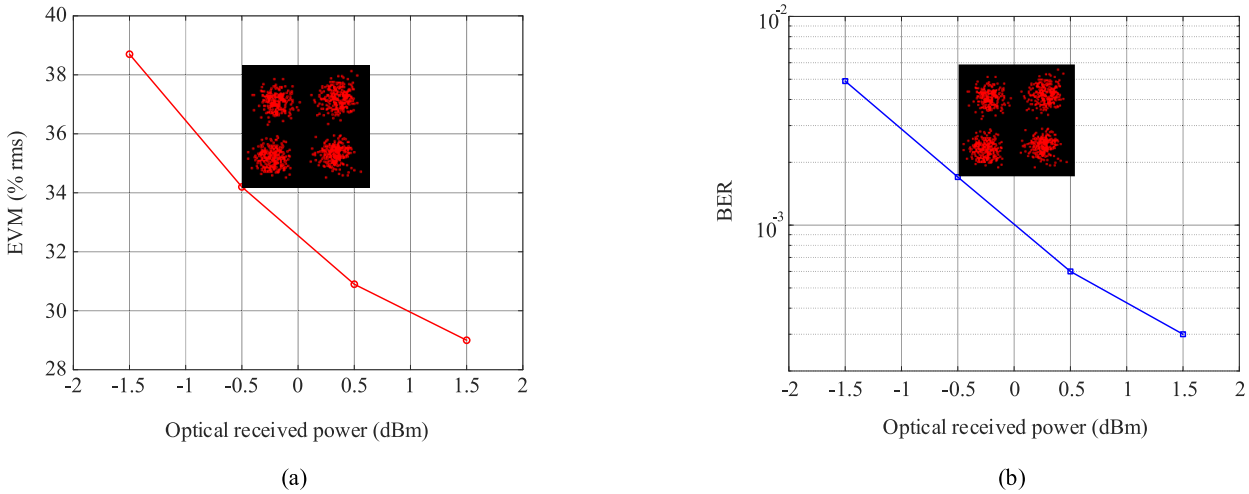

FIGURE 10. a) EVM and (b) BER versus the optical received power for QPSK converted THz signal over a hybrid transmission (15 km SMF and 1 m wireless channel).

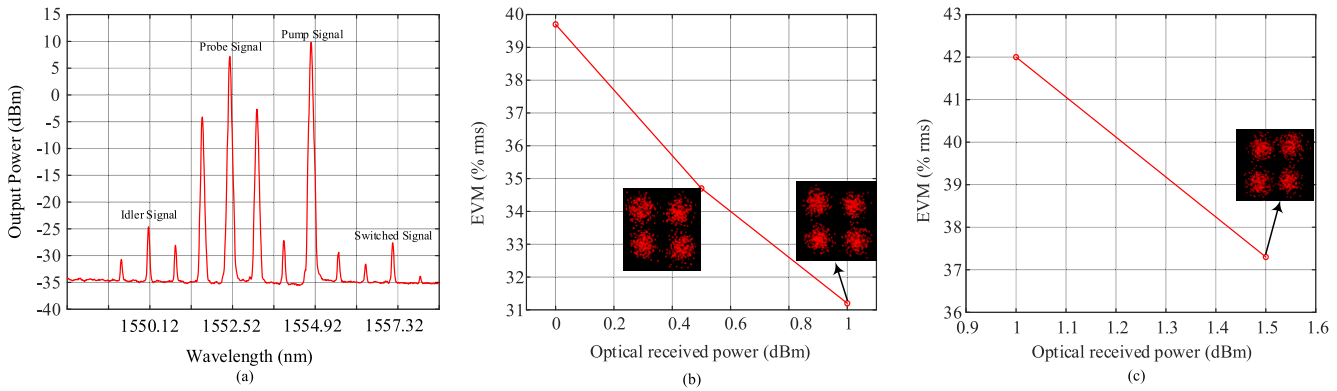

FIGURE 11. (a) Optical spectrum of SOA's output for up-conversion. (b-c) Up-conversion EVM versus the optical received power for QPSK converted THz signal over (b) BtB configuration, and (c) a hybrid transmission (15 km SMF and 0.5 m wireless channel).

using two horn antennas (SAGE SAR-2507-28-S2) over a wireless RF channel of 1 m length.

To study the wavelength conversion performance of the switched signal, we measure the error vector magnitude (EVM) and BER of the THz switch signal and the probe signal versus the optical received power in BtB configuration using a digital signal oscilloscope (Infiniium DSO-X-93204A). Figure 9 illustrates the EVM and BER of the THz signal and the probe signal. The threshold value of the FEC limit for QPSK signals is 37%. As shown in Fig. 9(a), the FEC limit can be achieved at −5.6 dBm optical received power in the case of the switched signal and −9 dBm in the case of the probe signal. This means a 3.4 dB power penalty. Fig. 9(b) displays the BER measurements, where the power penalty is 3.4 dB as well at the FEC limit. It should be noted that the variation in receiver sensitivity observed between the simulation and experimental results was attributed to the introduction of noise from electrical equipment such as AWG and DSO, along with optical devices including EDFAs and PD.

In addition to the BtB measurements, we considered transmitting the THz signal over a hybrid transmission link that includes 15 km SMF and 1 m wireless channel. Figure 10 illustrates the EVM and BER measurements versus the optical received power for the QPSK switched THz signal. As we can see, the QPSK signal transmission was successful and the FEC limit is obtained at −1.2 dBm optical received power.

The previous discussion considered the down-conversion of the switched signal. The next discussion considers the up conversion, where the pump signal has a higher wavelength than the probe signal. We set the wavelength of the probe signal at 1552.52 nm and the pump signal at 1554.92 nm. In this case, the switched signal is generated at 1557.32 nm wavelength. Figure 11(a) illustrates the output spectrum of the SOA in the case of up-conversion.

The EVM measurements of the switched THz signal in the case of up-conversion have been studied in two scenarios: BtB and a hybrid link that includes a 0.5 m wireless channel and transmission over 15 km SMF. The

results are illustrated in Fig. 11 (b) for BtB transmission and Fig. 11(c) for the transmission over the hybrid link. The results show a degradation in the performance of the up-conversion as compared to the down-conversion. Note that the maximum wireless channel is 0.5 m in the case of up-conversion, while in down-conversion, we easily reached to 1 m wireless channel. This degradation is because the contributing mechanisms to the FWM process such as carrier density modulation and spectral hole burning have phases that destructively interfere. In the up-conversion process, destructive interference occurs when two waves are completely out of phase, meaning a peak of one wave aligns with a trough of the other wave. Specifically, when two waves are out of phase by 180 degrees, they interfere destructively, resulting in cancellation of their amplitudes. In the down-conversion process, constructively interfering occurs when two waves having the same phase interact in such a way that they are aligned, leading to a new wave that has larger magnitude than either of the original waves. As a result, this enhances the conversion efficiency in down-conversion, thereby leading to an increase in the SSR. Theoretical analysis and experimental validation in [20], [28], [48], and [49] have demonstrated this phenomenon.

IV. CONCLUSION

This research demonstrated the feasibility of THz signal switching through both simulations and experiments. The experimental setup successfully transmitted 4 Gbps QPSK signals at a frequency of 100 GHz over a hybrid 15 km SMF and 1 meter RF channel. The FEC limit was achieved at −5.6 dBm optical received power, which represented a 3.4 dB power penalty compared to the probe signal. Additionally, the results indicated a performance degradation in the up-conversion process compared to down-conversion, which resulted in a reduced RF link length. The experimental setup served as a proof-of-concept, showing the feasibility of THz signal switching and transmission. Due to space limitations and the available hardware in our laboratory, we utilized a 1-meter wireless channel. Future work will address the analysis of longer distances, which could offer valuable insights into the performance and limitations of our approach in broader settings.

REFERENCES

[1] A. M. Ragheb, H. E. Seleem, A. S. Almaiman, and S. A. Alshebeili, "Reconfigurable photonics-based millimeter wave signal aggregation for non-orthogonal multiple access," *Opt. Exp.*, vol. 30, no. 10, pp. 16812–16826, 2022.

[2] T. Ha, A. Masood, W. Na, and S. Cho, "Intelligent multi-path TCP congestion control for video streaming in Internet of Deep Space Things communication," *ICT Exp.*, vol. 9, no. 5, pp. 860–868, Oct. 2023.

[3] C. V. N. Index, "Cisco visual networking index: Forecast and methodology 2015–2020," CISCO, San Jose, CA, USA, White paper, 2015.

[4] *Cisco Visual Networking Index: Forecast and Trends 2017-2022*, Cisco, San Jose, CA, USA, 2017.

[5] R. Li, "Towards a new internet for the year 2030 and beyond," in *Proc. 3rd Annu. ITU IMT-2020/5G Workshop Demo Day*, 2030, p. 121.

[6] H. Zhang, L. Zhang, and X. Yu, "Terahertz band: Lighting up next-generation wireless communications," *China Commun.*, vol. 18, no. 5, pp. 153–174, May 2021.

[7] C. D. López, "THz ultra-wideband passive devices: Design, simulation and characterization," M.S. thesis, Chalmers Tekniska Hogskola, Gothenburg, Sweden, 2021.

[8] X. Ma, Z. Chen, W. Chen, Z. Li, Y. Chi, C. Han, and S. Li, "Joint channel estimation and data rate maximization for intelligent reflecting surface assisted terahertz MIMO communication systems," *IEEE Access*, vol. 8, pp. 99565–99581, 2020.

[9] M. Pengnoo, M. T. Barros, L. Wuttisittikulkij, B. Butler, A. Davy, and S. Balasubramaniam, "Digital twin for metasurface reflector management in 6G terahertz communications," *IEEE Access*, vol. 8, pp. 114580–114596, 2020.

[10] C. Han, Y. Wu, Z. Chen, and X. Wang, "Terahertz communications (TeraCom): Challenges and impact on 6G wireless systems," 2019, *arXiv:1912.06040*.

[11] W. Yang and Y.-S. Lin, "Tunable metamaterial filter for optical communication in the terahertz frequency range," *Opt. Exp.*, vol. 28, no. 12, p. 17620, 2020.

[12] A. Singh, M. Andrello, N. Thawdar, and J. M. Jornet, "Design and operation of a graphene-based plasmonic nano-antenna array for communication in the terahertz band," *IEEE J. Sel. Areas Commun.*, vol. 38, no. 9, pp. 2104–2117, Sep. 2020.

[13] M. Civas and O. B. Akan, "Terahertz wireless communications in space," 2021, *arXiv:2110.00781*.

[14] A. Medlej, E. Dedu, K. Beydoun, and D. Dhoutaut, "Self-configuring asynchronous sleeping in heterogeneous networks," *ITU J. Future Evolving Technol.*, vol. 2, no. 7, pp. 51–62, 2021.

[15] Y. Wu, J. Koch, M. Vossiek, and W. Gerstacker, "Hierarchical beam alignment in SU-MIMO terahertz communications," *ITU J. Future Evolving Technol.*, vol. 2, no. 7, pp. 63–80, 2021.

[16] M. Sung, S.-R. Moon, E.-S. Kim, S. Cho, J. K. Lee, S.-H. Cho, T. Kawanishi, and H.-J. Song, "Design considerations of photonic THz communications for 6G networks," *IEEE Wireless Commun.*, vol. 28, no. 5, pp. 185–191, Oct. 2021.

[17] A. Tsakyridis, M. Moralis-Pegios, C. Vagionas, E. Ruggeri, G. Mourgias-Alexandris, A. Miliou, and N. Pleros, "Theoretical and experimental analysis of burst-mode wavelength conversion via a differentially-biased SOA-MZI," *J. Lightw. Technol.*, vol. 38, no. 17, pp. 4607–4617, May 18, 2020.

[18] S. Pan and J. Yao, "Photonics-based broadband microwave measurement," *J. Lightw. Technol.*, vol. 35, no. 16, pp. 3498–3513, Aug. 15, 2016.

[19] K. Iga and Y. Kokubun, *Encyclopedic Handbook of Integrated Optics*. Boca Raton, FL, USA: CRC Press, 2018.

[20] D. Zhu, Z. Wei, H. Wu, and S. Pan, "Photonics-based microwave switching using optical single sideband wavelength conversion in a semiconductor optical amplifier," *IEEE Trans. Microw. Theory Techn.*, vol. 65, no. 1, pp. 245–252, Jan. 2017.

[21] T. Nagatsuma, G. Ducournau, and C. C. Renaud, "Advances in terahertz communications accelerated by photonics," *Nature Photon.*, vol. 10, no. 6, pp. 371–379, Jun. 2016.

[22] M. Moralis-Pegios, N. Terzenidis, G. Mourgias-Alexandris, K. Vyrsokinos, and N. Pleros, "A 1024-port optical uni- and multicast packet switch fabric," *J. Lightw. Technol.*, vol. 37, no. 4, pp. 1415–1423, Jan. 21, 2019.

[23] M. Spyropoulou, N. Pleros, K. Vyrsokinos, D. Apostolopoulos, M. Bougioukos, D. Petrantonakis, A. Miliou, and H. Avramopoulos, "40 Gb/s NRZ wavelength conversion using a differentially-biased SOA-MZI: Theory and experiment," *J. Lightw. Technol.*, vol. 29, no. 10, pp. 1489–1499, Apr. 5, 2011.

[24] Parashuram and C. Kumar, "Optimal wavelength conversion of 250 Gbps PDM-(DP) QPSK signals based on dual SOA using co-polarized dual pumped FWM," *J. Opt.*, vol. 53, no. 2, pp. 1–21, 2024.

[25] H. Termos, A. Tharthar, and A. Mansour, "All-optical simultaneous frequency metamorphose contingent on a three parallel SOA-MZIs copula," *Optics*, vol. 4, no. 1, pp. 55–65, Jan. 2023.

[26] S. Matsuo and H. Uenohara, "Wide wavelength selectable and high frequency precision of all-optical wavelength conversion using pump light generated from optical combs and SSB modulation," *J. Lightw. Technol.*, vol. 40, no. 21, pp. 7006–7013, Aug. 11, 2022.

[27] D. Yang, Y. Guo, W. Chen, Y. Wu, K. Zhai, X. Wang, J. Cui, H. Wen, and C. Wang, "Ultrahigh efficiency four-wave mixing wavelength conversion in packaged silica microrod resonator," *J. Lightw. Technol.*, vol. 41, no. 6, pp. 1768–1774, Dec. 15, 2022.

[28] Y. Alkhlefat, A. M. Ragheb, M. A. Esmail, S. A. Alshebeili, and H. E. Seleem, "Millimeter wave switching for single carrier and aggregated filter bank multi-carrier signals in radio over fiber networks," *Opt. Fiber Technol.*, vol. 60, Dec. 2020, Art. no. 102335.

[29] F. Saadaoui, M. Fathallah, A. M. Ragheb, M. I. Memon, H. Fathallah, and S. A. Alshebeili, "Optimizing OSSB generation using semiconductor optical amplifier (SOA) for 5G millimeter wave switching," *IEEE Access*, vol. 5, pp. 6715–6723, 2017.

[30] F. D. Mahad, A. S. M. Supa'at, S. M. Idrus, and D. Forsyth, "Analyses of semiconductor optical amplifier (SOA) four-wave mixing (FWM) for future all-optical wavelength conversion," *Optik*, vol. 124, no. 1, pp. 1–3, Jan. 2013.

[31] Y. Alkhlefat, S. M. Idrus, and F. M. Iqbal, "Numerical analysis of UFMC and FBMC in wavelength conversion for radio over fiber systems using semiconductor optical amplifier," *Alexandria Eng. J.*, vol. 61, no. 7, pp. 5371–5381, Jul. 2022.

[32] M. A. Esmail, A. Ragheb, H. Fathallah, and S. Alshebeili, "Demonstration of photonics-based switching of 5G signal over hybrid all-optical network," *IEEE Photon. Technol. Lett.*, vol. 30, no. 13, pp. 1250–1253, May 29, 2018.

[33] Y. Alkhlefat, S. M. I. Sutan Nameh, and F. M. Iqbal, "Optimization of system's parameters for wavelength conversion of E-band signals," *Int. J. Electr. Comput. Eng.*, vol. 12, no. 2, p. 1659, Apr. 2022.

[34] G. Li, J. Li, G. Chen, and X. Huang, "SOA-based AOWC of 128QAM using Gaussian pulse shaping for transmission system with 227 gbps," *Microw. Opt. Technol. Lett.*, vol. 60, no. 9, pp. 2204–2216, Sep. 2018.

[35] K. Digambar and R. K. Jeyachitra, "An efficient photonic-based millimeter wavelength switching techniques towards 5G," in *Proc. Int. Conf. Wireless Commun., Signal Process. Netw. (WiSPNET)*, Mar. 2018, pp. 1–5.

[36] S.-H. Lee and J.-I. Song, "An XPolM-based all-optical SSB frequency up-conversion technique in an SOA," *IEEE Photon. Technol. Lett.*, vol. 29, no. 7, pp. 627–630, Mar. 1, 2017.

[37] Y. Al-Khlefat, S. M. Idrus, and M. A. Iqbal, "Generation of optical single side band signal using semiconductor optical amplifier for 5G signal," in *Proc. IEEE Photon. Conf. (IPC)*, Oct. 2021, pp. 1–2.

[38] Y. A. Alkhlefat, A. Ragheb, M. A. Esmail, and S. Alshebeili, "Millimeter wave switching in radio over fiber networks using semiconductor optical amplifier (SOA)," in *Proc. 21st Saudi Comput. Soc. Nat. Comput. Conf. (NCC)*, Apr. 2018, pp. 1–5.

[39] H.-J. Kim, H.-J. Song, and J.-I. Song, "All-optical frequency up-conversion technique using four-wave mixing in semiconductor optical amplifiers for radio-over-fiber applications," in *IEEE MTT-S Int. Microw. Symp. Dig.*, Jun. 2007, pp. 67–70.

[40] M. Matsuura and N. Kishi, "High-speed wavelength conversion of RZ-DPSK signal using FWM in a quantum-dot SOA," *IEEE Photon. Technol. Lett.*, vol. 23, no. 10, pp. 615–617, Feb. 24, 2011.

[41] H. Termos, "Study of up & down conversion technique by all-optical sampling based on SOA-MZI," Nat. School Eng. Brest (ENIB), Université de Bretagne occidentale-Brest, Brest, France, Tech. Rep., 2017.

[42] R. Gutierrez-Castrejon, L. Schares, L. Occhi, and G. Guekos, "Modeling and measurement of longitudinal gain dynamics in saturated semiconductor optical amplifiers of different length," *IEEE J. Quantum Electron.*, vol. 36, no. 12, pp. 1476–1484, Dec. 2000.

[43] G. Contestabile, A. Maruta, S. Sekiguchi, K. Morito, M. Sugawara, and K. Kitayama, "80 Gb/s multicast wavelength conversion by XGM in a QD-SOA," in *Proc. 36th Eur. Conf. Exhib. Opt. Commun.*, Sep. 2010, pp. 1–3.

[44] H. N. Tan, M. Matsuura, and N. Kishi, "Reduction of FWM and XGM for dynamic range improvement in SOA-based multiwavelength amplification using holding beam," in *Proc. OECC Tech. Dig.*, Jul. 2010, pp. 192–193.

[45] T. T. Ng, A. Perez, S. Sales, D. J. Richardson, and P. Petropoulos, "Characterization of XGM and XPM in a SOA-MZI using a linear frequency resolved gating technique," in *Proc. IEEE Lasers Electro-Opt. Soc. Annu. Meeting Conf.*, Oct. 2007, pp. 656–657.

[46] P. P. Baveja, D. N. Maywar, A. M. Kaplan, and G. P. Agrawal, "Self-phase modulation in semiconductor optical amplifiers: Impact of amplified spontaneous emission," *IEEE J. Quantum Electron.*, vol. 46, no. 9, pp. 1396–1403, Sep. 2010.

[47] D. Wu, L. Shen, H. Ren, M. Huang, C. Lacava, J. Campling, S. Sun, T. W. Hawkins, U. J. Gibson, P. Petropoulos, J. Ballato, and A. C. Peacock, "Four-wave mixing-based wavelength conversion and parametric amplification in submicron silicon core fibers," *IEEE J. Sel. Topics Quantum Electron.*, vol. 27, no. 2, pp. 1–11, Mar. 2021.

[48] D. F. Geraghty, R. B. Lee, M. Verdiell, M. Ziari, A. Mathur, and K. J. Vahala, "Wavelength conversion for WDM communication systems using four-wave mixing in semiconductor optical amplifiers," *IEEE J. Sel. Topics Quantum Electron.*, vol. 3, no. 5, pp. 1146–1155, Oct. 1997.

[49] J. Zhou, N. Park, J. W. Dawson, K. J. Vahala, M. A. Newkirk, and B. I. Miller, "Efficiency of broadband four-wave mixing wavelength conversion using semiconductor traveling-wave amplifiers," *IEEE Photon. Technol. Lett.*, vol. 6, no. 1, pp. 50–52, Jan. 1994.

YAZAN ALKHLEFAT received the B.S. degree from AL Yarmouk University, Jordan, in 2011, the master's degree from King Saud University, Saudi Arabia, in 2019, and the Ph.D. degree from Universiti Teknologi Malaysia, Malaysia, in December 2023. Since 2018, he has been with NOKIA as a Senior Microwave Transmission Planning Consultant for 4G and 5G projects at STC Operator. He has been with HUAWEI as a Microwave Transmission Engineer for 4G projects at STC Operator, from 2013 to 2018. From 2011 to 2013, he was with STC Operator as a NOC Engineer. His research interests include photonic-MMW and sub-terahertz systems, 5G networks and their modulation formats, and semiconductor optical amplifier devices.

MAGED A. ESMAIL received the B.E. degree in electronic engineering from Ibb University, in 2006, and the M.Sc. and Ph.D. degrees (Hons.) in electrical engineering from KSU University, in 2012 and 2017, respectively. He was a Postdoctoral Research Associate with the KACST-TIC RFTONICS Center, King Saud University. He is currently an Associate Professor of electrical engineering with Prince Sultan University, Saudi Arabia. He has served as a reviewer for various IEEE journals and other international journals. He has authored/co-authored more than 90 journal and conference publications. His research interests include optical communications, photonic-based radars, machine learning applications for optical communication, the IoT, and 5G networks. He serves as an Associate Editor for IEEE Access journal.

AMR M. RAGHEB was a full-time Researcher with the Prince Sultan Advanced Technology Research Institute (PSATRI), Riyadh, Saudi Arabia, in 2012. He was a full-time Researcher with the Digital Photonic Test Division, Keysight Technologies, Boeblingen, Germany, in 2013. He is currently an Associate Professor with the Electrical Engineering Department, King Saud University, where he is also the Director of the Photonics Laboratory, Technology Innovation Center in RF and Photonics (RFTONICS), College of Engineering, King Saud University. He has more than 12 years of experience with the Photonics Telecommunication Laboratory. His research interests include photonic-microwave integration, quantum dash-based lasers, free-space optical communications, optical modulation format identification, and sub-terahertz systems.

SEVIA MAHDALIZA IDRUS (Senior Member, IEEE) received the bachelor's degree in electrical engineering and the master's degree in engineering management from UTM, in 1998 and 1999, respectively, and the Ph.D. degree in optical communication engineering from the University of Warwick, U.K., in 2004. Since 1998, she has been with UTM as an Academic and Administrative Staff. She was appointed as a Guest Professor with Osaka Prefecture University and Tokai University, Japan, in 2011 and 2014, respectively. Her research output has been translated into a number of publications (H-index-17) and IPR, including a high-end reference book, 'Optical Wireless Communication: IR Connectivity'published by Taylor and Francis, 49 book chapters and monographs, more than 200 refereed research articles, eight patents granted, 36 patent filings and holds 31 UTM copyrights. Her main research interests include optical communication system and networks, optoelectronic design, and engineering management. She is a member of the Editorial Board of a few refereed international journals.

FARABI M. IQBAL received the M.Eng. degree in electronics and telecommunications from Universiti Teknologi Malaysia, and the Ph.D. degree in optical networking from the Delft University of Technology, The Netherlands. He is currently a Senior Lecturer with the School of Electrical Engineering, Universiti Teknologi Malaysia, where he has been a Faculty Member, since 2009. His research interests include network routing, resiliency, and optimization.

SALEH A. ALSHEBEILI was the Chairperson of the Electrical Engineering Department, King Saud University, Riyadh, Saudi Arabia, from 2001 to 2005. He has more than 30 years of teaching and research experience in the area of communications and signal processing. He was a member of the Board of Directors with the King Abdullah Institute for Research and Consulting Studies, from 2007 to 2009, and a member of the Board of Directors with the Prince Sultan Advanced Technologies Research Institute, from 2008 to 2017, where he was the Managing Director, from 2008 to 2011, and the Director of the Saudi-Telecom Research Chair, from 2008 to 2012. He has been the Director of the Technology Innovation Center, RF and Photonics in e-Society, funded by King Abdulaziz City for Science and Technology (KACST), since 2011. He is currently a Professor with the Electrical Engineering Department, King Saud University, and a member of the Spectrum Advisory Group formed by the Communications, Space, and Technology Commission, Saudi Arabia.